

Article

A Light-Weighted Machine Learning Approach to Channel Estimation for New-Radio Systems

Hyun Woo Lee  and Sang Won Choi * 

Department of Electronic Engineering, Kyonggi University, Suwon 16227, Republic of Korea; hwlee16@kyonggi.ac.kr

* Correspondence: swchoi20@kyonggi.ac.kr

Abstract: In this paper, we provide a light-weighted Machine Learning (ML) approach to channel estimation for New-Radio (NR) systems. Specifically, based on the equivalence between the Channel Impulse Response (CIR) in the time domain and its corresponding Channel Frequency Response (CFR) in the frequency domain, the light-weighted ML model for the channel estimation is shown to be established in comparison to the existing ML-based channel estimator. Furthermore, for practical use, the quantized weights for the light-weighted ML-based estimator are shown to be feasible without significant performance degradation in the sense of mean square error (MSE), which shows the effectiveness of the proposed approach from the perspective of memory overhead. Consequently, we show that there exists Signal to Noise Ratio (SNR) gain in comparison with the existing ML-based estimator, which is validated by numerical results considering the Sounding Reference Signal (SRS) for NR in the 3rd Generation Partnership Project (3GPP).

Keywords: channel estimation; Channel Impulse Response (CIR); Channel Frequency Response (CFR); Machine Learning (ML); New-Radio (NR); quantization; Sounding Reference Signal (SRS); 3rd Generation Partnership Project (3GPP)



Citation: Lee, H.W.; Choi, S.W. A Light-Weighted Machine Learning Approach to Channel Estimation for New-Radio Systems. *Electronics* **2023**, *12*, 4740. <https://doi.org/10.3390/electronics12234740>

Academic Editor: Xiongwen Zhao

Received: 30 October 2023

Revised: 17 November 2023

Accepted: 20 November 2023

Published: 22 November 2023



Copyright: © 2023 by the authors. Licensee MDPI, Basel, Switzerland. This article is an open access article distributed under the terms and conditions of the Creative Commons Attribution (CC BY) license (<https://creativecommons.org/licenses/by/4.0/>).

1. Introduction

Orthogonal Frequency Division Multiple Access (OFDMA), an MA scheme for New-Radio (NR), has gained widespread adoption in wireless communication systems owing to its resilience against frequency-selective fading channels. The receiver in wireless communication receives a distorted signal due to delay spread, which is the multipath effect. Therefore, the channel must be estimated to compensate for the distorted signal. In general, channels are estimated using pilot signals known to both the transmitter and receiver. Since the pilot signals used vary depending on the user scenario, channels are estimated by generating signals such as the Demodulation Reference Signal (DMRS) [1] and Sounding RS (SRS) [2–5].

Existing channel estimation methods usually estimate channels using the Least Square (LS) and Minimum Mean Square Error (MMSE). The LS method estimates the channel by assuming that the channel is deterministic. Specifically, the LS uses only pilot signals except for the channel's statistical information and the computational complexity is quite low. However, the statistical information of the channel is not used, so the performance is relatively low from the perspective of MSE. The MMSE method utilizes the statistical information of the channel to exhibit optimal performance from the MSE perspective. However, there is a disadvantage that optimal performance can be achieved only when the statistical information of the channel is properly known, and the computational complexity is relatively high compared to the LS method. It is necessary to study an improved channel estimation method to compensate for the problems of these existing channel estimation methods.

On the other hand, a variety of Machine Learning (ML)-based estimation methods have been studied to compensate for the shortcomings of existing estimation methods.

Table 1 depicts representative studies [6–16] conducted for achieving comparable performance to the MMSE method using ML without the statistical information of the channel in comparison with main contributions from this study. It is noteworthy to design the channel estimation method using the black-box characteristic of ML. However, ML-based Channel Frequency Response (CFR) estimation methods have the disadvantage of high complexity because inputs and outputs are proportional to the length of the pilot signal, and the number of hidden layers is typically large. In the case of ML-based Channel Impulse Response (CIR) estimation, it is complicated to use because the channel is estimated at each time instance of the received signal in the time domain, or the received signal in the frequency domain is estimated through multiple MLs. Furthermore, memory overhead is likely to occur as memory requirements to store ML increase in proportion to the number of hidden layers and nodes.

Table 1. A concise comparison of our work with the existing ML-based channel estimations.

Perspective	Contents
Input data type in ML	<ul style="list-style-type: none"> · Machine learning using received signal [6] · Machine learning using estimated channels [7–13] · Machine learning using transmitted and received signals [14] · Machine learning using transmitted signal, received signal, and estimated channels [15,16]
Design the number of usage symbols according to channel types	<ul style="list-style-type: none"> · ML to estimate instantaneous channels from one symbol [6–9,16] · ML to estimate the channel for the current symbol using the channel estimated from the previous symbol [10,11,14,15] · ML to perform interpolation to estimate the channel of the slot where pilot symbols are located not only that of the pilot symbol [12,13]
Channel estimation by domain types	<ul style="list-style-type: none"> · Estimation of Channel Impulse Response in time domain [14,16] · Estimation of Channel Frequency Response in frequency domain [6–13,15]
Complexity and MSE performance	<ul style="list-style-type: none"> · Low complexity and low MSE performance due to the use of simple ML structure (with or without one hidden layer) [8,16] · High complexity and high MSE performance from leveraging complicated ML structure (MNN or CNN, LSTM, and so on) [6,7,9–15]
Our work	<ul style="list-style-type: none"> · Estimation of channel impulse response using received signal in the frequency domain · Single slot design for channel estimation with a one-time symbol · Low complexity and high MSE performance with the simple ML structure

In this paper, we propose a memory-saving ML-based channel estimation for estimating CIR with low complexity. The ML model adopts Deep Neural Networks (DNNs) to design as simple as possible with one hidden layer, and it uses ML's black box characteristics to input received signals in the frequency domain and output CIR in the time domain. The weights of the trained ML can be stored by converting them from floating point 32 to integral point 8 using the weight quantization method [17,18].

The rest of this paper is organized as follows. The system model for the process before using the channel estimation method is introduced in Section 2. The existing channel estimation and the simplest ML-based CFR estimation are presented in Section 3. The proposed method in a general environment is presented in Section 4. A simulation analysis of the proposed method and simulation analyses based on additional perspectives are presented in Section 5. Our main conclusion is given in Section 6.

Notations: Vectors and matrices are written in bold letters. $\mathbb{E}[\mathbf{X}]$ is the expectation of the random vector \mathbf{X} . $(\cdot)^T$ and $(\cdot)^\dagger$ represent transpose and Hermitian transpose, respectively. $\|\mathbf{x}\|$ and \otimes are the norm of the vector \mathbf{x} and convolution, respectively. $\lfloor x \rfloor$ is the nearest integer to x , and $Re(\mathbf{x})$ and $Im(\mathbf{x})$ are real and imaginary values of the vector \mathbf{x} , respectively.

2. System Model

This paper considers the comb-type pilot arrangement-based OFDM system [19–22] with K_{TC} intervals for subcarriers of length N_{sc} , as shown in Figure 1. Figure 2 shows a typical block

diagram of the OFDM system with the pilot signal assisted. $\bar{\mathbf{S}} = [S_0, \dots, S_{N-1}]^T$ is an $N \times 1$ pilot signal vector known by both transmitters and receivers, and $\bar{\mathbf{X}} = [X_0, \dots, X_{N_{sc}-1}]^T$ is an $N_{sc} \times 1$ transmission signal vector in a frequency domain where pilot signal $\bar{\mathbf{S}}$ is placed at regular intervals in subcarriers, and symbols without pilot signals are set to 0. After pilot insertion, $\bar{\mathbf{X}}$ adds the $N_{zp} \times 1$ Zero Padding (ZP) vector $\mathbf{0}_{N_{zp}}$ to both sides to expand to the $N_{fft} \times 1$ vector, and as shown in Equation (1), $\bar{\mathbf{X}}$ with ZP added is sent to an N_{fft} -point Inverse Fast Fourier Transform (IFFT), which is modulated into \mathbf{x} in the time domain as

$$\mathbf{x} = \mathbf{F}_{N_{fft}}^{-1}[\mathbf{0}_{N_{zp}}, \bar{\mathbf{X}}, \mathbf{0}_{N_{zp}}]^T, \tag{1}$$

where $\mathbf{F}_{N_{fft}}^{-1}$ is an N_{fft} -point IFFT matrix and $N_{zp} = \frac{1}{2}(N_{fft} - N_{sc})$.

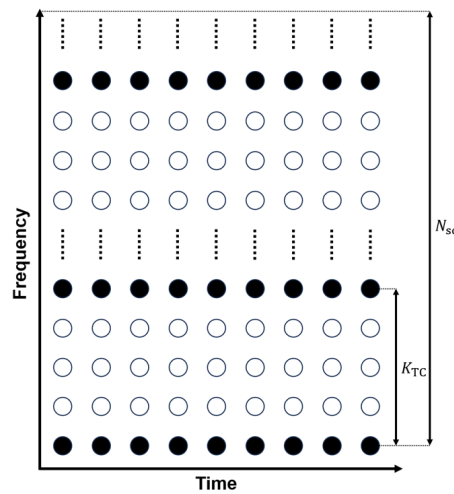


Figure 1. Comb-type pilot arrangement for OFDM ($K_{TC} = 4$).

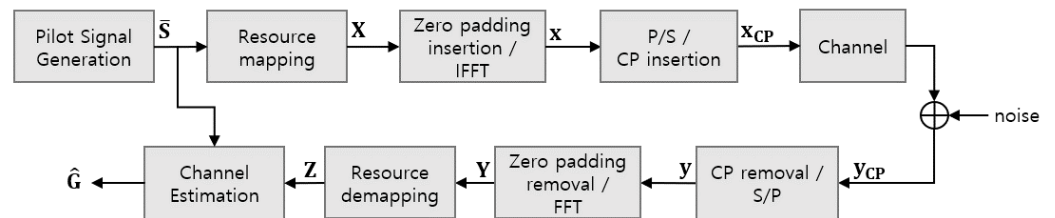


Figure 2. Block diagram in OFDM for channel estimation.

The transmission signal \mathbf{x} places a cyclic-prefix (CP) of length N_{cp} at the front of the signal to prevent Inter-Symbol Interference (ISI), and then a $(N_{fft} + N_{cp}) \times 1$ vector \mathbf{x}_{cp} is transmitted to the receiver. Assuming that the channel is invariant over the duration of the OFDM symbol and is in perfect synchronization, the received signal \mathbf{y}_{cp} is written as

$$\mathbf{y}_{cp} = \mathbf{x}_{cp} \otimes \mathbf{h} + \mathbf{n}_{cp}, \tag{2}$$

where $\mathbf{h} = [h_0, h_1, \dots, h_{L-1}]^T$ is an $L \times 1$ CIR vector generated by Gaussian random variables, and \mathbf{n}_{cp} is a $(N_{fft} + N_{cp}) \times 1$ vector, which is Additive White Gaussian Noise (AWGN) with zero mean and variance σ_n^2 .

When sampling for the received signal is completed, N_{fft} -point FFT is performed after removing the CP for demodulation. Therefore, the FFT output for the received signal is expressed as

$$\mathbf{Y} = \mathbf{X}\mathbf{H} + \mathbf{w}, \tag{3}$$

where \mathbf{X} is an $N_{sc} \times N_{sc}$ diagonal matrix containing the transmitted signal. \mathbf{H} is an $N_{sc} \times 1$ CFR vector and \mathbf{w} is an $N_{sc} \times 1$ i.i.d. complex Gaussian random vector with zero mean and variance σ_n^2 . The n -th component of CFR H_n is expressed as [23]

$$H_n = FFT\{\mathbf{h}\} = \sum_{l=0}^{L-1} h_l e^{-j2\pi ln/N_{fft}}, \quad (4)$$

$$0 \leq n \leq N_{fft} - 1.$$

Since the transmission signal is concentrated on the pilot symbol-based method through the reference signal, it is written with the received signal and CFR for the subcarrier containing the pilot as

$$\mathbf{Z} = \mathbf{S}\mathbf{G} + \bar{\mathbf{w}}, \quad (5)$$

where \mathbf{Z} and \mathbf{G} are $N \times 1$ vectors that are CFR and received signals for pilot subcarriers, respectively. \mathbf{S} is the $N \times N$ diagonal matrix of the reference signal according to \mathbf{Z} , and $\bar{\mathbf{w}}$ represents $N \times 1$ i.i.d. complex Gaussian random vectors with zero mean and variance σ_n^2 . Consequently, the channel estimation method is performed through Equation (5).

3. Preliminaries on Channel Estimation

3.1. LS/MMSE Method

Using the $N \times 1$ reference signal vector \mathbf{S} for the received signal \mathbf{Z} , we perform the LS method and estimate the channel as follows

$$\begin{aligned} \hat{\mathbf{G}}_{LS} &= \mathbf{S}^{-1}\mathbf{Z} \\ &= \mathbf{S}^{-1}(\mathbf{S}\mathbf{G} + \bar{\mathbf{w}}) \\ &= \mathbf{G} + \mathbf{S}^{-1}\bar{\mathbf{w}} \\ &= \mathbf{G} + \tilde{\mathbf{w}} \end{aligned} \quad (6)$$

where $\tilde{\mathbf{w}}$ represents $N \times 1$ i.i.d. complex Gaussian random vectors with vectors zero mean and variance $\sigma_n^2/\mathbb{E}\{\mathbf{S}\mathbf{S}^\dagger\}$. As shown in Equation (6), the LS method is one of the most common approaches because of the simple calculation. However, it is difficult to make precise channel estimation because $\tilde{\mathbf{w}}$ remains in the estimated channel, and it does not use the statistical information of the channel. Therefore, to overcome the limitations of the LS method and minimize mean square errors, the MMSE method is performed as follows

$$\hat{\mathbf{G}}_{MMSE} = R_{GZ}R_{ZZ}^{-1}\mathbf{Z}, \quad (7)$$

where $R_{GZ} = \mathbb{E}\{\mathbf{G}\mathbf{Z}^\dagger\}$ is an $N \times N$ cross-correlation matrix between the channel and received signal, and $R_{ZZ} = \mathbb{E}\{\mathbf{Z}\mathbf{Z}^\dagger\}$ is the $N \times N$ auto-correlation matrix for the received signal. The MMSE method may improve channel estimation accuracy by using the statistical information of the channel. However, it has a higher computational complexity than the LS method and requires statistical information of the channel. Additionally, there is a limitation in using the MMSE method because it may be difficult to obtain channel information, and accurate information is not guaranteed.

3.2. Existing ML Method

3.2.1. Structure

To compensate for the shortcomings of existing channel estimators, ML-based channel estimation that performs as well as the MMSE method without utilizing the statistical information of the channels is being studied. Figure 3 shows the simplest form of the ML method [7] among the existing ML methods used to compare with the proposed method in this paper. The ML-aided channel estimation is designed to minimize the MSE between the actual channel and the estimated channel obtained by the LS method to overcome the LS and MMSE methods, and the number of nodes in the input layer and output layer is

2N. The number of hidden layers is 3, and the number of nodes in the hidden layers is designed to be 4N. In detail, the input data use the estimated CFR \hat{G}_{LS} by the LS method, and when these input data are input to the ML, the ML outputs a new estimated CFR \hat{G}_{ML} corresponding to \hat{G}_{LS} . Since the ML does not accept complex numbers, \hat{G}_{LS} must be input by dividing it into real and imaginary numbers and \hat{G}_{ML} is also output divided into real and imaginary numbers as follows

$$\mathbf{X}_{in,d} = \begin{bmatrix} Re(\hat{G}_{LS,d}(0)) \\ Im(\hat{G}_{LS,d}(0)) \\ \vdots \\ Re(\hat{G}_{LS,d}(N-1)) \\ Im(\hat{G}_{LS,d}(N-1)) \end{bmatrix},$$

$$\mathbf{Y}_{out,d} = \begin{bmatrix} Re(\hat{G}_{ML,d}(0)) \\ Im(\hat{G}_{ML,d}(0)) \\ \vdots \\ Re(\hat{G}_{ML,d}(N-1)) \\ Im(\hat{G}_{ML,d}(N-1)) \end{bmatrix},$$

$$d = \{1, \dots, D\},$$
(8)

where N is the length of the pilot signal, and $\mathbf{X}_{in,d}$ and $\mathbf{Y}_{out,d}$ are the input and output for the d-th data, respectively. Since the $\mathbf{Y}_{out,d}$ output by the ML is divided into real and imaginary numbers, it is converted to a complex number to obtain $\hat{G}_{ML,d} = [\hat{G}_{ML,d}(0), \dots, \hat{G}_{ML,d}(N-1)]^T$.

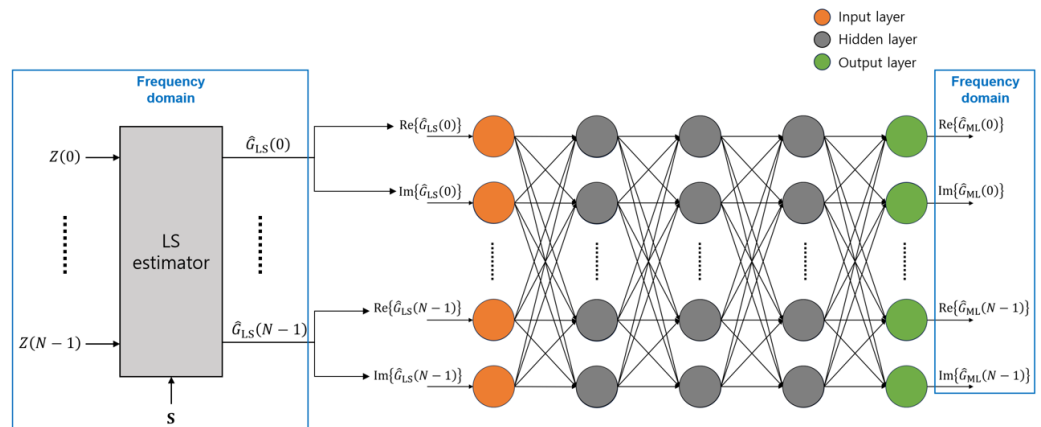


Figure 3. The structure of the existing ML-based channel estimator.

3.2.2. Activation Function

The m' -th node of the k -th hidden layer performs the following calculations:

$$o_{k,m'} = f_{m'}(z) = f_{m'}\left(\sum_{m=1}^M w_m x_m + b_m\right),$$

$$k = \{1, 2, 3\},$$

$$m' = \{1, \dots, M'\},$$
(9)

where M is the number of inputs ($m = 1, \dots, M$) to the m -th node in the previous layer, and M' is the number of nodes in the current hidden layer. w_m is the m -th weight and b_m is the bias. $f(\cdot)$ is the activation function used to characterize the nonlinearity of the channel

data, and $o_{k,m'}$ is the output for the m' -th node of the k -th hidden layer. In this model, the activation function of the hidden layer adopts the tanh function as

$$f(z) = \frac{e^z - e^{-z}}{e^z + e^{-z}}, \tag{10}$$

where e is Euler’s number. The output $\hat{G}_{ML,d}$ for the d -th data is obtained in ML from the input $\hat{G}_{LS,d}$ and uses the loss function to minimize the MSE between the prediction channel and the actual channel as follows

$$\mathcal{L}(\mathcal{W}, \mathcal{B}) = \frac{1}{DN} \sum_{d=1}^D \sum_{n=0}^{N-1} \|G_d(n) - \hat{G}_{ML,d}(n)\|^2, \tag{11}$$

where $G_d(n)$ is the actual channel value associated with $\hat{G}_{ML,d}(n)$, and \mathcal{W} and \mathcal{B} include all the weights and biases, respectively. From a set of initial values, the weights and biases are updated by minimizing the loss function shown in Equation (10).

Since ML-aided channel estimation is based on LS estimates, it minimizes the MSE between actual channels, so it performs better than the LS method, but there are three hidden layers, and each node is designed twice the input size, resulting in high complexity. Therefore, we propose a low-complexity ML-based channel estimation where ML designed the DNN with a single hidden layer. We also propose weight quantization that can save memory stored by reducing the capacity of weights.

4. Proposed ML Method

4.1. Network Architecture

4.1.1. Structure

To compensate for the shortcomings of LS, MMSE, and existing ML-based channel estimation, we propose a CIR estimation that is closer to the actual channel than the LS method and requires no prior information, unlike the MMSE method. Figure 4 shows the structure of the proposed ML-based channel estimation, which includes a DNN architecture. To propose the low-complexity ML, it is designed with only one hidden layer and estimates a CIR shorter than CFR.

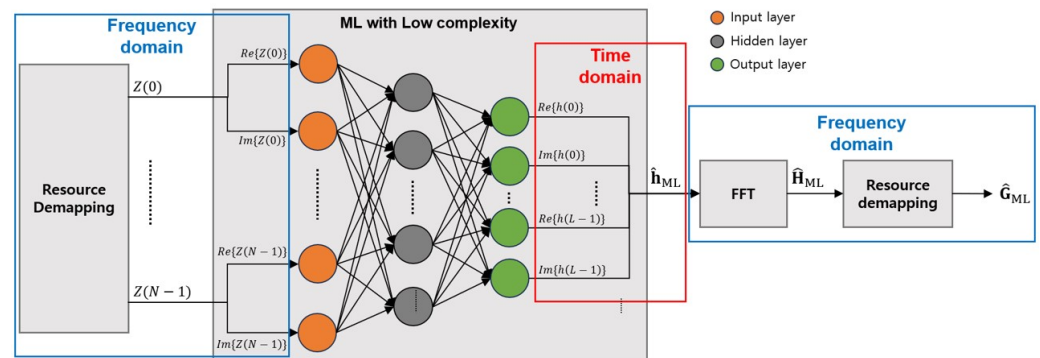


Figure 4. The structure of the proposed ML-based channel estimator.

The receiver receives transmission signals coming through channels in various directions. Therefore, the reception signal can be expressed as the convolution product of the channel impulse response and the transmission signal, and the first part of the reception signal is affected by the reception signal of the previous symbol, resulting in Inter-Symbol Interference. Accordingly, the communication system prevents Inter-Symbol Interference by adding a CP in front of the transmission signal. In general, since the length of the channel impulse response is smaller than the CP, ISI prevention is possible. Long pilot signals are transmitted for more accurate channel estimation, but too-long pilot signals generate overhead. The pilot signal has an appropriate length and thus occurs longer than

the length of the channel impulse response. Consequently, the L -length CIR output from the proposed ML is shorter than the N -length CFR output from the existing ML, and a simpler ML can be designed.

It is necessary to distinguish between real and imaginary parts of the complex signal because the current ML platform only allows real numbers. Therefore, the input data of the ML for the d -th data $\mathbf{X}_{in,d}$ are given as follows

$$\mathbf{X}_{in,d} = \begin{bmatrix} \text{Re}(Z_d(0)) \\ \text{Im}(Z_d(0)) \\ \vdots \\ \text{Re}(Z_d(N-1)) \\ \text{Im}(Z_d(N-1)) \end{bmatrix}. \tag{12}$$

The number of nodes in the output layer is $2L$ according to the length of CIR L , and the output value of the ML for the d -th data $\mathbf{Y}_{out,d}$ is given as follows

$$\mathbf{Y}_{out,d} = \begin{bmatrix} \text{Re}(\hat{h}_d(0)) \\ \text{Im}(\hat{h}_d(0)) \\ \vdots \\ \text{Re}(\hat{h}_d(L)) \\ \text{Im}(\hat{h}_d(L)) \\ \vdots \\ \text{Re}(\hat{h}_d(L-1)) \\ \text{Im}(\hat{h}_d(L-1)) \end{bmatrix}, \tag{13}$$

where $\hat{h}_d(l) (l = 0, \dots, L)$ is the output of the neural network for the l -th tap of the d -th data. The number of nodes in the hidden layer is less than the number of pilot signals N and the largest is the power of 2, and it is represented by $Q = 2^{\lceil \log_2(N) \rceil}$. Since the objective of ML-based estimation is to minimize the MSE between the estimated channel and the actual channel, the loss function \mathcal{L} used in the training step is defined as follows

$$\mathcal{L}(\mathcal{W}, \mathcal{B}) = \frac{1}{DL} \sum_{d=1}^D \sum_{l=0}^{L-1} \|h_d(l) - \hat{h}_d(l)\|^2, \tag{14}$$

where D is the number of data used for training, and $h_d(l)$ is the actual channel value associated with $\hat{h}_d(l)$. From a set of initial values, the weights and biases are updated by minimizing the loss function shown in Equation (13) with the forward and backward propagation.

The proposed method estimates the CIR, so the CIR is converted into the CFR to derive the pilot symbol-based CFR $\hat{\mathbf{G}}_{ML}$ as follows

$$\begin{aligned} \hat{\mathbf{H}}_{ML} &= \mathbf{F}_{N_{fft}} \cdot [\hat{\mathbf{h}}_{ML}, \mathbf{0}_{N_{fft}-L}]^T, \\ \hat{\mathbf{G}}_{ML} &= \hat{\mathbf{H}}_{ML}(\text{idx}(\mathbf{S})), \end{aligned} \tag{15}$$

where $\mathbf{0}_{N_{fft}-L}$ is the $(N_{fft} - L) \times 1$ zero vector, and $\mathbf{F}_{N_{fft}}$ is the N_{fft} -point FFT matrix. $\text{idx}(\mathbf{S})$ refers to the location where the pilot signal is placed on the subcarrier.

4.1.2. Activation Function

Since there is only one hidden layer of the proposed method, nodes are defined as follows

$$o_{m'} = f_{m'}(z) = f_{m'}\left(\sum_{m=1}^M w_m x_m + b_m\right). \tag{16}$$

Since the purpose of the proposed method is to reduce complexity using the simple DNN, the activation function of the DNN $f(\cdot)$ uses the tanh function shown in Equation (9)

the closer the input is to zero. The greater the differential value, the more easily it is able to converge and complete the training quickly. The tanh function is shown in Figure 5. As shown in Figure 5a, the output of the function is in the $[-1, 1]$ interval and the median is 0, so there is no bias. Additionally, since the gradient is mostly steep and can be both positive and negative, it quickly converges to the optimal value and has almost no gradient loss, as shown in Figure 5b.

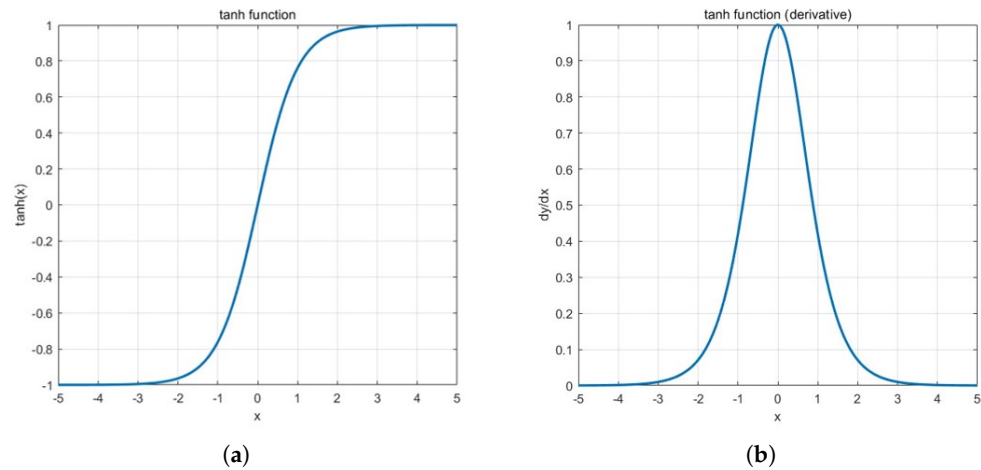


Figure 5. (a) The tanh function, (b) derivative of tanh function.

4.1.3. Complexity Analysis

In this paper, we compare computational complexity through the number of multiplications for the existing methods and the proposed method. The computational complexity of the existing ML and the proposed ML add the LS method for the input data $\hat{\mathbf{G}}_{LS}$ and the N_{fft} point FFT to transform from CIR to CFR, respectively. The results are shown in Table 2, where $Q = 2^{\lceil \log_2(N) \rceil}$ is the largest power of 2, while it is less than N . Here, N_{fft} is the FFT size. In addition, N and L are the pilot signal size and the length of the CIR, respectively. These results show that the existing ML is lower than the MMSE method and slightly higher than the LS method, but the proposed ML is lower than the LS method as well as the MMSE method.

Table 2. Computational complexity of ML-based estimators with LS and MMSE.

Algorithm	The Number of Multiplications/Inversions	Computational Complexity
LS	$N^2 + N$	$O(N^2)$
MMSE	$N^3 + 3N^2$	$O(N^3)$
Existing ML	$N^2 + N + 2N \times 4N + 3 \times (4N \times 4N) + 4N \times 2N$ $= 65N^2 + N$	$O(N^2)$
Proposed ML	$2N \times Q + Q \times 2L + N_{fft} \times L$ $= 2Q(N + L) + N_{fft} \times L$	$O(QN)$

4.2. Quantization Method

The trained ML performs a quantization of 32-bit floating-point weights \mathbf{w} to 8-bit integer-point weights for the interval $[-128, 127]$, as shown in Figure 6. For quantization, values that are 32 bits are divided into a certain range to quantize them into 8 bits. In this figure, different proximity weight values, such as w_{k-1} and w_k , are quantized to the same value if they belong to the same interval when quantized to 8 bits. Different weight values within the interval are quantized to the same value, so performing inverse quantization to use ML converts them to the same weight value. Therefore, when the weights go through quantization, they are set to a value different from the original value, resulting in performance loss. The maximum value w_{max} and minimum value w_{min} of

\mathbf{w} are stored in memory for dequantization. Then, when using the proposed ML for channel estimation, quantized weights must be applied to ML after dequantization. The dequantization normalizes the interval $[-128, 127]$ with stored w_{\max} and w_{\min} to derive the interval $[w_{\min}, w_{\max}]$.

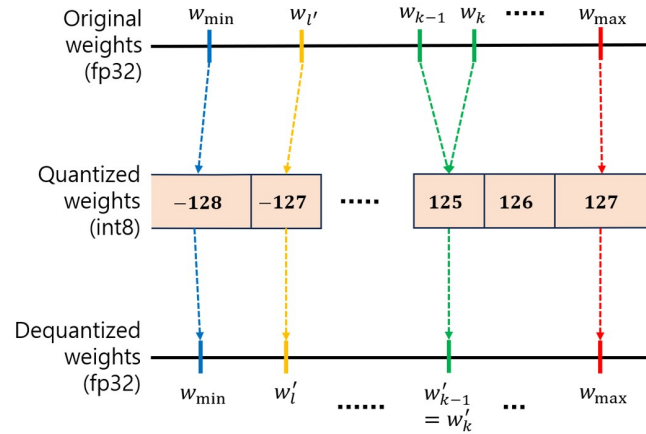


Figure 6. The structure of the weight quantization algorithm.

In the case of weight quantization for memory saving, w_{\max} and w_{\min} must be stored because it is to be restored based on them. However, if the length of the CIR is $L = 1$ and $L = 6$, then each cumulative distribution function (CDF) of the proposed ML for the weights \mathbf{w} is shown in Figure 7. As shown in this figure, the probability that the value of $|w|$ exists below 0.5 is $F(w) = P(|w| \leq 0.5) > 0.99$. Therefore, almost all the weights are assigned within the interval $[-0.5, 0.5]$, and the dequantization step uses the interval $[-0.5, 0.5]$ to dequantize the interval $[-128, 127]$ instead of using w_{\max} and w_{\min} for memory saving.

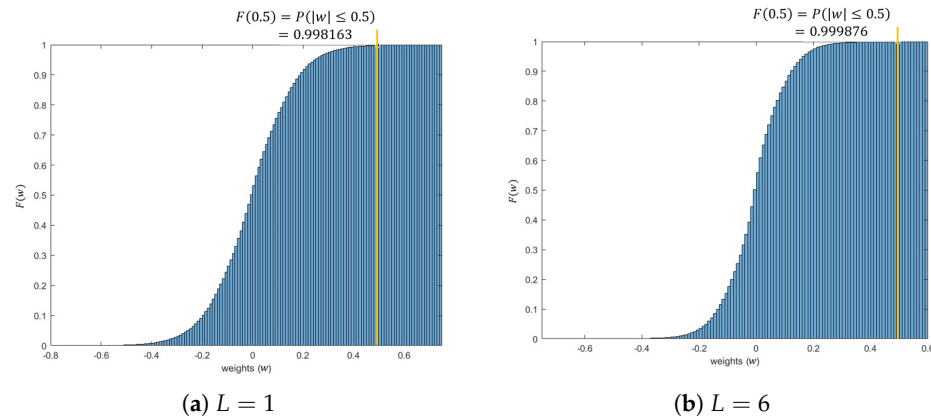


Figure 7. CDF of weights for the proposed ML.

5. Simulation Analysis

5.1. Simulation Environment

In this paper, the environment for channel estimation is based on the pilot signal generated through the 5G NR Sounding Reference Signal (SRS) [24]. In 5G NR, the OFDM system is almost the same as the OFDM system in LTE [25], so it is possible to follow the system model in Section 2. SRS is generated based on the Low Peak to Average Power Ratio (PAPR) sequence as follows

$$r_{u,v}^{(\alpha,\delta)}(n) = e^{j\alpha n} \bar{r}_{u,v}(n), \quad 0 \leq n \leq M_{sc}^{RS}, \tag{17}$$

where $M_{sc}^{RS} = mN_{sc}^{RB}/2^\delta$ is the length of the SRS, and m is the number of resource blocks (RBs) occupied by the SRS. N_{sc}^{RB} is the number of subcarriers contained in one RB, and δ is $\delta = \log_2(K_{TC})$ according to transmission comb number $K_{TC} \in \{2, 4, 8\}$. The base sequence $\bar{r}_{u,v}(n)$ depends on the group number u and the number of base sequences v , and multiple orthonormal SRS can be generated using different cyclic shift α even with the same base sequence.

For $M_{ZC} \geq 3N_{sc}^{RB}$, the base sequence $\bar{r}_{u,v}(n)$ ($0 \leq n \leq M_{sc}^{RS}$) is given by

$$\begin{aligned}\bar{r}_{u,v}(n) &= x_q(n \bmod N_{ZC}), \\ x_q(m) &= e^{-j\frac{\pi qm(m+1)}{N_{ZC}}},\end{aligned}\quad (18)$$

where q is given by

$$\begin{aligned}q &= \lfloor \bar{q} + 1/2 \rfloor + v \cdot (-1)^{\lfloor 2\bar{q} \rfloor}, \\ \bar{q} &= N_{ZC} \cdot (u + 1) / 31.\end{aligned}\quad (19)$$

The length N_{ZC} is given by the largest prime number such that $N_{ZC} < M_{sc}^{RS}$.

To evaluate the performance of the proposed ML-based channel estimation in this paper, an algorithm for channel estimation was designed using MATLAB (R2021b)-based simulation [26], and the parameters used in the simulation are shown in Table 3. The correlation matrices of the MMSE method design an ideal MMSE using the actual CFR \mathbf{G} . Parameters required for the proposed ML are shown in Table 4. As an additional technique, ML utilizes an Adam optimizer to quickly reach global optimum points without converging to local optimum points [27]. The structure of the layer in the proposed ML is designed as shown in Table 5. The performance of the ML is verified after the training is completed. In this simulation, the CIR was set in consideration of the AWGN channel with $L = 1$ and the multipath channel with $L = 6$, wherein the power of each component of the CIR is the same and the sum is 1. The trained ML performs weight quantization for the weights in the ML, and quantized weights are stored in memory.

Table 3. The parameters for OFDM system.

Parameters	Values
SRS size (N)	48
Subcarrier size (N_{sc})	216
FFT size (N_{fft})	256
Tap size (L)	1, 6
Channel model	Gaussian channel
Noise model	Gaussian noise
SNR	$[-10 : 5 : 20]$

Table 4. The parameters for proposed ML.

Parameters	Values
Number of hidden layer	1
Input layer size ($2N$)	96
Hidden layer size (Q)	32
Output layer size ($2L$)	2, 12
Batch size	8
Learning rate	10^{-4}
Training epochs	100
Activation function	tanh
Optimizer	Adam
Loss function	Mean squared error

Table 5. The structures of each layer for the proposed ML.

Layers	1Tap DNN		6Tap DNN	
	Nodes	$f(\cdot)$	Nodes	$f(\cdot)$
Input layer	96	-	96	-
Hidden layer	32	tanh	32	tanh
Output layer	2	-	12	-

The performance metric between the actual channel and the estimated channel was verified using the MSE defined as follows in Equation (20) for each signal-to-noise ratio (SNR)

$$MSE = \frac{1}{IN} \sum_{i=1}^I \sum_{n=0}^{N-1} \|G_i(n) - \hat{G}_i(n)\|^2, \tag{20}$$

where $G_i(n)$ is the actual channel for the n -th component of the i -th iteration, and $\hat{G}_i(n)$ is also the estimated channel for the component corresponding to $G_i(n)$.

5.2. Simulation Results

5.2.1. Comparison between Existing Methods and Proposed Method

Figure 8 compares the MSE performance of the proposed channel estimation method with the two lengths of the CIR scenarios. Figure 8a,b show the length of the CIR at $L = 1$ and $L = 6$, respectively. The performance of the proposed method is compared to the LS, MMSE, and existing ML methods, and all methods improve their performance as the SNR increases. In both scenarios, the LS methods do not take advantage of the statistical information of the channel, resulting in the worst MSE performance. On the other hand, the performance of the MMSE method is better than the LS method in both scenarios, because the MMSE method uses the statistical information of the channel. The existing ML methods and the proposed methods performed better than the LS methods in both scenarios. However, the performance of the existing ML method is better than the MMSE method below about 7 dB in the $L = 1$ scenario, but it reverses above 7 dB. And it is worse than the MMSE method at all the SNRs in the $L = 6$ scenario. The performance of the proposed method without performed weight quantization is better than the MMSE method at all the SNRs in the $L = 1$ scenario but is worse than the MMSE method at all the SNRs in the $L = 6$ scenario. Both the existing and proposed MLs suffer performance degradation depending on the length of the CIR, which is estimated to reduce ML’s computational accuracy as the received signal becomes complex due to the convolutional multiplication of the transmitted signal. Furthermore, the performance degradation is expected to be due to the fact that the received signal information does not increase proportionally with the length of the CIR, but rather the longer CIR must be inferred from the same amount of received signal information, leading to more challenging results.

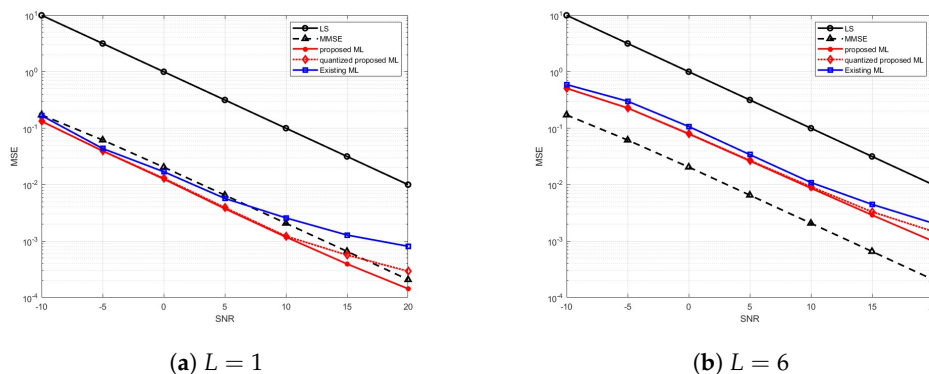


Figure 8. Performance comparison between existing methods and the proposed method.

Meanwhile, it outperforms the existing ML method in both scenarios like the proposed method without the quantization. The quantized ML methods have no differences in performance from the proposed ML methods without performing weight quantization below the SNR of 10 dB in both scenarios. It is also observed that there are slight performance differences in the SNR regime which is greater than or equal to 10 dB, but it remained better than the existing ML methods.

5.2.2. The Number of Hidden Layers

To ensure the reliability of the proposed method of designing only one hidden layer, the proposed method is designed with three hidden layers like the existing ML method and compared with the one-hidden-layer method. As shown in Figure 9, there are little differences between proposed algorithms with 1 and 3 hidden layers in both scenarios. Therefore, it can be seen that the proposed method can be efficiently designed to complete the training quickly by reducing the complexity of ML by setting one hidden layer rather than slightly increasing the performance by setting a lot of hidden layers. Although the performance loss for weight quantization appears to occur similarly in both methods, the performance becomes unstable as the number of hidden layers increases, as shown in the $L = 6$ scenario.

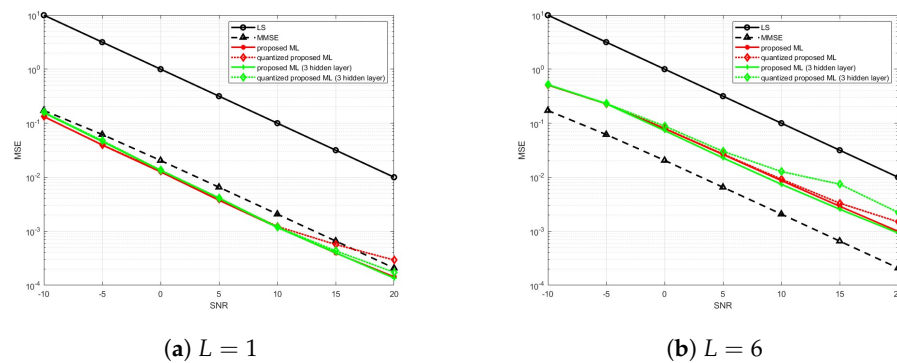


Figure 9. Performance comparison between proposed algorithms with 1 and 3 hidden layers.

5.2.3. ML Robustness to Other SNRs

As shown in Figure 10, the model of the proposed method was trained with only the set SNR, and the performance is compared by entering data for each SNR. In both scenarios, there is little performance loss compared to the correct trained models for each SNR. Moreover, in the $L = 1$ scenario, below about 10 dB, the model trained with 10 dB data performs better than that trained with 20 dB data, but above about 10 dB, the model trained with 20 dB data performs better than that trained with 10 dB data. Consequently, the proposed method is robust against other SNR data, as there is little performance loss even if SNR data different from that of the trained data are inputted.

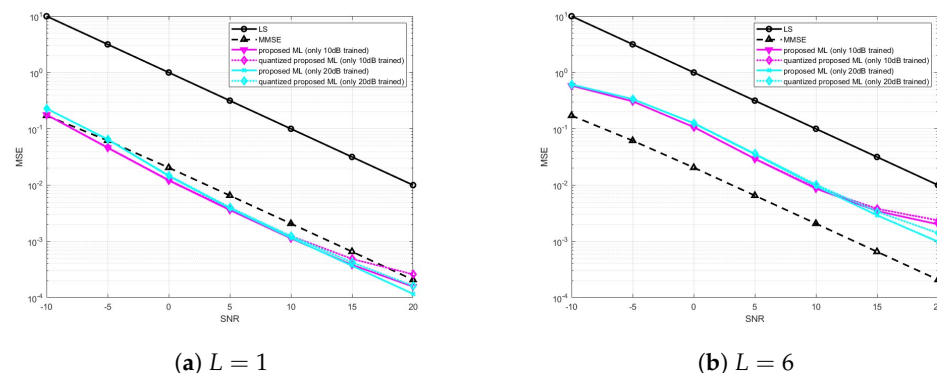


Figure 10. Performance based on different SNR data than the trained SNR data.

6. Conclusions

In this paper, we provided the light-weighted ML approach to channel estimation for NR systems. The main intuition was that there exists an equivalence between the CIR in the time domain and its corresponding CFR in the frequency domain. Based on the CFR rather than the CIR, it was shown that the more light-weighted ML model can be established in comparison with the existing ML-based channel estimator. Specifically, regardless of the number of CIR's channel taps, it was observed that the ML model configuration with one input layer, one hidden layer, and one output layer was sufficient to learn the channel estimation, which was confirmed from the computational complexity comparison in Table 2. Furthermore, the proposed light-weighted ML-based channel estimator was shown to be robust when the quantized weights were applied to reduce memory overhead, which opened the availability for practical use. From the perspective of the MSE performance, the proposed ML-based estimator has better performance than the existing ML-based channel estimator. One interesting thing is that the proposed ML-based estimator had better performance even than MMSE when the number of channel taps is equal to 1, which showed the effectiveness of the proposed one especially for poor scattering channel environments. Instead of naive use of the proposed ML-based estimator training for each SNR, it was observed that with a trained proposed ML-based estimator, the specific SNR is sufficient to cover all the SNR regimes without significant performance degradation. As a further work, the proposed ML-based estimator can be naturally extended to CFR interpolation based on the inference of the CIR, which can be further elaborated.

Author Contributions: Conceptualization, H.W.L. and S.W.C.; methodology, H.W.L. and S.W.C.; software, H.W.L.; validation, H.W.L. and S.W.C.; formal analysis, H.W.L. and S.W.C.; investigation, H.W.L.; resources, H.W.L.; data curation, H.W.L.; writing—original draft preparation, H.W.L.; writing—review and editing, S.W.C.; visualization, H.W.L.; supervision, S.W.C.; project administration, H.W.L. and S.W.C.; funding acquisition, S.W.C. All authors have read and agreed to the published version of the manuscript.

Funding: This work was supported by the Institute of Information & Communications Technology Planning & Evaluation (IITP) grant funded by the Korea government (MSIT). (No. 2021-0-00165, Development of 5G+ Intelligent Base Station Software Modem).

Institutional Review Board Statement: Not applicable.

Informed Consent Statement: Not applicable.

Data Availability Statement: Data are contained within the article.

Conflicts of Interest: The authors declare no conflict of interest.

Abbreviations

The following abbreviations are used in this manuscript:

3GPP	3rd Generation Partnership Project
5G	5th Generation
AWGN	Additive White Gaussian Noise
CFR	Channel Frequency Response
CIR	Channel Impulse Response
CNN	Convolutional Neural Network
CP	Cyclic-Prefix
DMRS	DeModulation Reference Signal
DNN	Deep NN
FFT	Fast Fourier Transform
IFFT	Inverse FFT
i.i.d.	Independent and Identically Distributed
LSTM	Long Short-Term Memory
ML	Machine Learning
MNN	Multi-Layer NN

MSE	Mean Square Error
NR	New-Radio
OFDMA	Orthogonal Frequency Division Multiple Access
PAPR	Peak-to-Average Power Ratio
SRS	Sounding Reference Signal
ZP	Zero Padding

References

- Hou, X.; Zhang, Z.; Kayama, H. DMRS Design and Channel Estimation for LTE-Advanced MIMO Uplink. In Proceedings of the 2009 IEEE 70th Vehicular Technology Conference Fall, Anchorage, AK, USA, 20–23 September 2009; pp. 1–5.
- Wang, Y.; Zheng, A.; Zhang, J.; Yang, D. A novel channel estimation algorithm for sounding reference signal in LTE uplink transmission. In Proceedings of the 2009 IEEE International Conference on Communications Technology and Applications, Beijing, China, 16–18 October 2009; pp. 412–415.
- Bertrand, P. Channel Gain Estimation from Sounding Reference Signal in LTE. In Proceedings of the 2011 IEEE 73rd Vehicular Technology Conference (VTC Spring), Budapest, Hungary, 15–18 May 2011; pp. 1–5.
- Xia, X.; Zhao, H.; Zhang, C. Improved SRS design and channel estimation for LTE-advanced uplink. In Proceedings of the 2013 5th IEEE International Symposium on Microwave, Antenna, Propagation and EMC Technologies for Wireless Communications, Chengdu, China, 29–31 October 2013; pp. 84–90.
- Tran, H.; Mai, T.-A.; Dang, S.; Ngo, H.-A. Large-scale MU-MIMO uplink channel estimation using sounding reference signal. In Proceedings of the 2018 2nd International Conference on Recent Advances in Signal Processing, Telecommunications & Computing (SigTelCom), Ho Chi Minh City, Vietnam, 29–31 January 2018; pp. 107–110.
- Balevi, E.; Doshi, A.; Andrews, J.G. Massive MIMO Channel Estimation With an Untrained Deep Neural Network. *IEEE Trans. Wireless Commun.* **2020**, *19*, 2079–2090. [[CrossRef](#)]
- Le Ha, A.; Van Chien, T.; Nguyen, T.H.; Choi, W. Deep Learning-Aided 5G Channel Estimation. In Proceedings of the 2021 15th International Conference on Ubiquitous Information Management and Communication (IMCOM), Seoul, Republic of Korea, 4–6 January 2021; pp. 1–7.
- Mei, K.; Liu, J.; Zhang, X.; Cao, K.; Rajatheva, N.; Wei, J. A Low Complexity Learning-Based Channel Estimation for OFDM Systems With Online Training. *IEEE Trans. Commun.* **2021**, *69*, 6722–6733. [[CrossRef](#)]
- Ma, X.; Gao, Z. Data-Driven Deep Learning to Design Pilot and Channel Estimator for Massive MIMO. *IEEE Trans. Veh. Technol.* **2020**, *69*, 5677–5682. [[CrossRef](#)]
- Jiang, P.; Wen, C.-K.; Jin, S.; Li, G. Y. Dual CNN-Based Channel Estimation for MIMO-OFDM Systems. *IEEE Trans. Commun.* **2021**, *69*, 5859–5872. [[CrossRef](#)]
- Le, H.A.; Van Chien, T.; Nguyen, T.H.; Choo, H.; Nguyen, V.D. Machine learning-based 5G-and-beyond channel estimation for MIMO-OFDM communication systems. *Sensors* **2021**, *21*, 4861. [[CrossRef](#)] [[PubMed](#)]
- Dayi, A.B. Improving 5G NR Uplink Channel Estimation with Artificial Neural Networks: A Practical Study on NR PUSCH Receiver. In Proceedings of the 2022 IEEE International Black Sea Conference on Communications and Networking (BlackSeaCom), Sofia, Bulgaria, 6–9 June 2022; pp. 129–134.
- Liao, Y.; Hua, Y.; Cai, Y. Deep Learning Based Channel Estimation Algorithm for Fast Time-Varying MIMO-OFDM Systems. *IEEE Commun. Lett.* **2020**, *24*, 572–576. [[CrossRef](#)]
- Bai, Q.; Wang, J.; Zhang, Y.; Song, J. Deep Learning-Based Channel Estimation Algorithm Over Time Selective Fading Channels. *IEEE Trans. Cognit. Commun. Netw.* **2019**, *6*, 125–134. [[CrossRef](#)]
- Yang, Y.; Gao, F.; Ma, X.; Zhang, S. Deep Learning-Based Channel Estimation for Doubly Selective Fading Channels. *IEEE Access* **2019**, *7*, 36579–36589. [[CrossRef](#)]
- Jebur, B.A.; Alkassar, S.H.; Abdullah, M.A.M.; Tsimenidis, C.C. Efficient Machine Learning-Enhanced Channel Estimation for OFDM Systems. *IEEE Access* **2021**, *9*, 100839–100850. [[CrossRef](#)]
- Han, S.; Mao, H.; Dally, W.J. Deep compression: Compressing deep neural networks with pruning, trained quantization and Huffman coding. *arXiv* **2015**, arXiv:1510.00149.
- Gholami, A.; Kim, S.; Dong, Z.; Yao, Z.; Mahoney, M.W.; Keutzer, K. A Survey of Quantization Methods for Efficient Neural Network Inference. *arXiv* **2021**, arXiv:2103.13630.
- van de Beek, J.-J.; Edfors, O.; Sandell, M.; Wilson, S.K.; Borjesson, P.O. On channel estimation in OFDM systems. In Proceedings of the 1995 IEEE 45th Vehicular Technology Conference. Countdown to the Wireless Twenty-First Century, Chicago, IL, USA, 25–28 July 1995; pp. 815–819.
- Hsieh, M.-H.; Wei, C.-H. Channel estimation for OFDM systems based on comb-type pilot arrangement in frequency selective fading channels. *IEEE Trans. Consum. Electron.* **1998**, *44*, 217–225. [[CrossRef](#)]
- Morelli, M.; Mengali, U. A comparison of pilot-aided channel estimation methods for OFDM systems. *IEEE Trans. Signal Process.* **2001**, *49*, 3065–3073. [[CrossRef](#)]
- Coleri, S.; Ergen, M.; Puri, A.; Bahl, A. Channel estimation techniques based on pilot arrangement in OFDM systems. *IEEE Trans. Broadcast.* **2002**, *48*, 223–229. [[CrossRef](#)]

23. Hajizadeh, R.; Mohamedpor, K.; Tarihi, M.R. Channel Estimation in OFDM System Based on the Linear Interpolation, FFT and Decision Feedback. In Proceedings of the 18th Telecommunication forum TELFOR 2010, Serbia, Belgrade, 23–25 November 2010.
24. 3GPP TS 38.211 v17.3.0; NR Physical Channels and Modulation. European Telecommunications Standards Institute: Sophia Antipolis, France, 2022.
25. Kumar T.A.; Anjaneyulu, L. Channel Estimation Techniques for Multicarrier OFDM 5G Wireless Communication Systems. In Proceedings of the 2020 IEEE 10th International Conference on System Engineering and Technology (ICSET), Shah Alam, Malaysia, 9 November 2020; pp. 98–101.
26. Cho, Y.S.; Kim, J.; Yang, W.Y.; Kang, C.G. *MIMO-OFDM Wireless Communications with MATLAB*; John Wiley & Sons: Hoboken, NJ, USA, 2010.
27. Kingma, D.P.; Ba, J. Adam: A method for stochastic optimization. *arXiv* **2014**, arXiv:1412.6980.

Disclaimer/Publisher’s Note: The statements, opinions and data contained in all publications are solely those of the individual author(s) and contributor(s) and not of MDPI and/or the editor(s). MDPI and/or the editor(s) disclaim responsibility for any injury to people or property resulting from any ideas, methods, instructions or products referred to in the content.